Study on the Applicability of k-ε Model to Nuclear Safety Problems

Gong Hee Lee [a]*, Ae Ju Cheong [b]
[a]*Korea Institute of Nuclear Safety, Daejon, 305-338*
[b]*Nuclear Safety Research Department, Korea Institute of Nuclear Safety, Daejon, 305-338*
[*]*Corresponding author: ghlee@kins.re.kr*

1. Introduction

Although the competitiveness of Computational Fluid Dynamics (CFD) is growing steadily due to rapid developments in computer hardware technology, computing capacity is still a limiting factor for CFD calculations to produce completely accurate results for the prediction of the nuclear safety-related flow phenomena. For example, Direct Numerical Simulation (DNS) require the excessive computing power, and thus, it is practically impossible for DNS to be used in the preliminary reactor design process. Therefore turbulence models are required to bridge the gap between the real flow and the statistically averaged equations.

Two equation models such as k-ε model, which use the eddy-viscosity assumption, are widely used for industrial CFD applications. They offer a good compromise between complexity, accuracy and robustness. However, this model cannot be expected to perform well in the cases such as impinging jets, flow separation in a strong adverse pressure gradient, strongly swirling flows and buoyant driven flow. A Reynolds Stress model may show the improved prediction for rotating flow, secondary flow and buoyant flow by solving a transport equation for the independent Reynolds stresses. However, this model can introduce a strong nonlinearity, giving rise to numerical problems in many applications.

Although recently licensing applications supported by using the commercial CFD software are increasing, there is no commercial CFD software which obtains a licensing from the domestic regulatory body until now. In addition, there is no domestic regulatory guideline for the comprehensive evaluation of CFD software. Therefore, from a regulatory perspective, Korea Institute of Nuclear Safety (KINS) is presently conducting the performance assessment of the commercial CFD software for nuclear reactor problems.

In this study, to assess the applicability of k-ε model to the typical nuclear safety problems such as the complex flow phenomena inside either the fuel assembly or the reactor vessel, simulation was performed using the commercial CFD software, ANSYS CFX R.14 [1] and the predicted results with k-ε model were compared with the measured data and the computational results with more complex turbulence models.

2. MATiS-H (KAERI)

2.1 Overview of Test Facility

MATiS-H test facility, installed in the KAERI (Korea Atomic Energy Research Institute), was used to perform hydraulic tests in a rod bundle array under the unheated conditions. As shown in Fig. 1, test rig consists mainly of a water storage tank, a circulation pump, and a test section.

The main body of the horizontal test section comprises a 4.67 m-long square duct of inner dimensions 0.17×0.17 m, containing a 3.863m-long 5×5 rod bundle array. Outer diameter of a fuel rod, rod-to-rod pitch, and rod-to-wall pitch were 25.4 mm, 33.12 mm, and 18.75mm, respectively. The hydraulic diameter (D_h) of the flow cross-section was 24.27 mm.

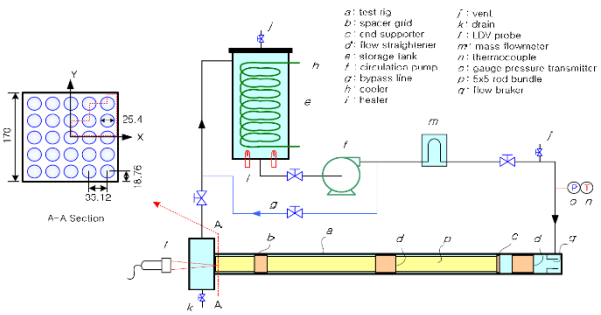

Fig. 1. Schematic diagram of test facility. [2]

As shown in Fig. 2, 'Split-type' spacer grid, which featured two vanes being bent through an angle of 30° with respect to the horizontal, was installed in the rod bundle for enhancing the lateral turbulent mixing in the subchannels.

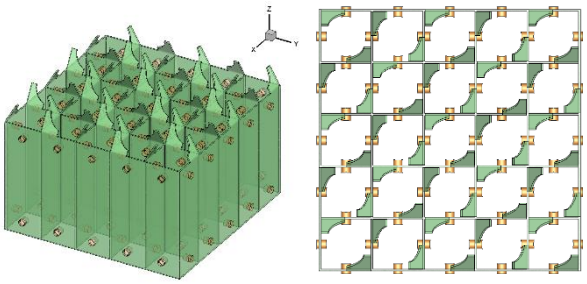

(a) Isometric view (b) Top view

Fig. 2. 'Split-type' spacer grid.

Detailed measurements of velocity components in subchannels have been obtained using a two-component LDA (Laser Doppler Anemometry) system at four

different axial locations (Z = 0.5, 1.0, 4.0 and 10D_h) from the downstream edge of the mixing vane tip. Turbulence intensities and vortices in the subchannels were then evaluated from the measured velocity components.

The combined uncertainties of the LDA velocity measurements for all lateral and axial components, normalized with respect to the axial bulk velocity, were estimated to be 4.8%~ 5.1% with 95% confidence.

2.2 Test Conditions

Light water at 35℃ and 156.9kPa was used as the working fluid. The mass flow rate was 24.2kg/s resulting in a bulk velocity of 1.5m/s. The Reynolds number based on the hydraulic diameter (D_h) was 50,250. The mean values and their uncertainties of test conditions are summarized in Table I.

Table I: Test Conditions. [2]

Parameters	Unit	Mean value	Uncertainty (%)
Mass flow rate	kg/s	24.2	0.29
Temperature	℃	35	2.90
Pressure	kPa	156.9	0.39
Bulk velocity	m/s	1.5	0.37
Reynolds number		50,250	2.01

2.3 Geometry Modeling

The original CAD file of the 'Split-type' spacer grids, provided by MATiS-H benchmark organizers, was used for the mesh generation. As shown in Fig. 3, only small gaps between rods and the so-called buttons (i.e. small cylinders used for spacer and rod fixation) were filled by projecting the buttons as solid cylinders flush with the rods because these gaps would not influence the flow distributions due to their small size and would require significantly higher effort to generate the fine mesh [3].

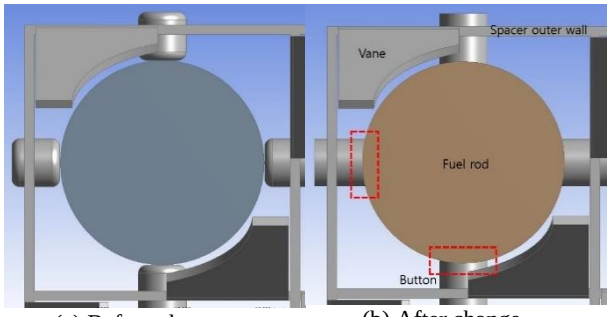

(a) Before change (b) After change

Fig. 3. Geometry simplification.

2.4 Numerical Modeling

2.4.1. Numerical method.

The flow inside the fuel assembly was assumed to be unsteady, incompressible, isothermal and turbulent. A high resolution scheme was used for the convection-terms-of-momentum and –turbulence equations. The 2nd Order Backward Euler scheme was used for the transient term. A time step of 0.001sec was used with the maximum 10 iterations per time step. Total simulation time was 3sec. The solution was considered 'converged' when the residuals of the variables were below 10^{-5} at each time step. Simulation was conducted with the commercial CFD software, ANSYS CFX R.14 [1].

2.4.2. Turbulence models.

Both k-ε model and SAS (Scale-Adaptive Simulation)-SST (Shear Stress Transport) model were used to simulate the turbulent flow inside the fuel assembly. For SAS-SST model, the information provided by the von Karman length-scale allows SAS models to dynamically adjust to resolved structures in URANS (Unsteady Reynolds Averaged Navier-Stokes) simulation, which results in a LES (Large Eddy Simulation)-like behavior in unsteady regions of the flow field. At the same time, the model provides standard RANS capabilities in stable flow regions. More detailed descriptions of SAS-SST model can be found in the ANSYS CFX-solver modeling guide [4].

2.4.3. Grid systems.

Fig. 4 shows the grid system for the computational domain that had the same size as the test facility. A hybrid mesh, made up of tetrahedrons, wedges, pyramids and hexahedrons, was generated to prevent the oversimplification of the geometry, and to have more efficient mesh distribution. Prism layers were used to get higher resolution in the near-wall region. Total numbers of elements were 1.7×10^7 and maximum y+ was 24.

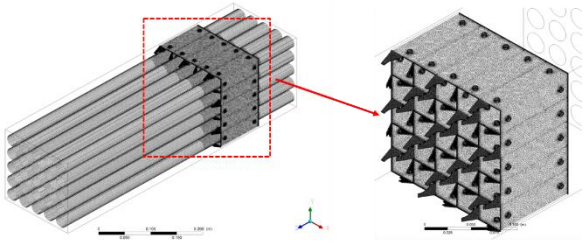

Fig. 4. Grid system.

2.4.4. Boundary conditions.

Fully developed cross sectional profiles of velocity components, obtained from corresponding precursor simulation on Z-periodic thin rod bundle, were used as an inlet boundary condition. Turbulence intensity at the inlet was assumed to be 5 %. The 'average pressure over the whole outlet' option; with a relative pressure of 0 Pa, was used as an outlet-boundary condition. A no-slip condition was applied at the solid wall. To model the

flow in the near-wall region, the scalable wall-function approach was used for the k-ε model. For SAS-SST model, automatic near-wall treatment was applied.

2.5 Results and Discussion

2.5.1. Time averaged velocity profiles.

Fig. 5 shows the time averaged horizontal, vertical and axial velocity profile respectively at Y=0.5P and two different axial locations, Z=0.5D_h and 4.0D_h, from the downstream edge of the mixing vane tip.

Because the location of a subchannel center was nearly same as that of the vortex center at Y=0.5P, the magnitudes of U/W_{bulk} and V/W_{bulk} were nearly zero. The flow direction was also changed at Y=0.5P & Z=0.5D_h and therefore U/W_{bulk} and V/W_{bulk} showed repeatedly the negative and positive magnitudes.

For the time averaged velocity components, prediction performance of k-ε model was at least equivalent to that of SAS-SST model except for the certain sections (for example, X/P=0~0.25 for U/W_{bulk}).

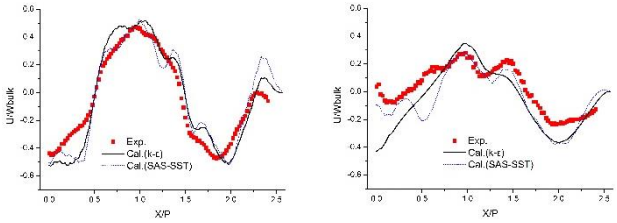

(a) Horizontal velocity (U/W_{bulk})

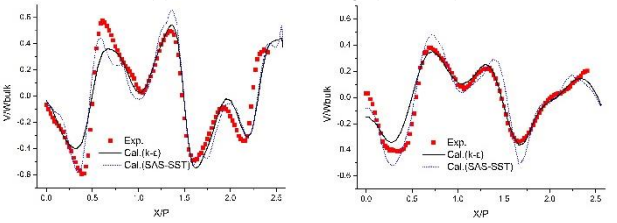

(b) Vertical velocity (V/W_{bulk})

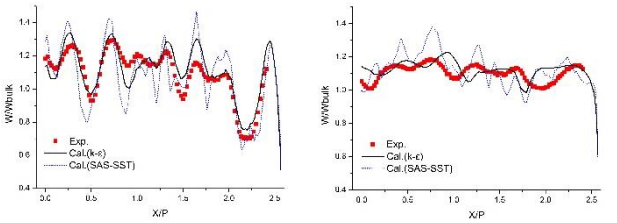

(c) Axial velocity (W/W_{bulk})

Fig. 5. Time averaged horizontal, vertical and axial velocity profiles at Y=0.5P (left : Z=0.5D_h, right : Z=4.0D_h).

2.5.2. Time averaged axial vorticity.

Fig. 6 shows the time averaged axial vorticity (ω_z) contour in the sub-channels at two different axial locations, Z=1.0 and 10.0D_h, from the downstream edge of the mixing vane tip. The time averaged axial vorticity can be defined by using the measured horizontal and vertical velocity in the subchannels as follows:

$$\omega_z = \left(\frac{\partial V}{\partial x} - \frac{\partial U}{\partial y}\right)$$

At Z=1.0D_h, the predicted axial vorticity with k-ε model showed that the positive peak magnitude regions in some sub-channels were more tilted to the horizontal direction and more flat pattern in comparison with the measurement.

On the other hand, k-ε model predicted the similar vorticity pattern to the measurement at Z=10.0D_h. However, the peak magnitude of vorticity was relatively decayed in comparison with the measurement due to the unique features of k-ε model.

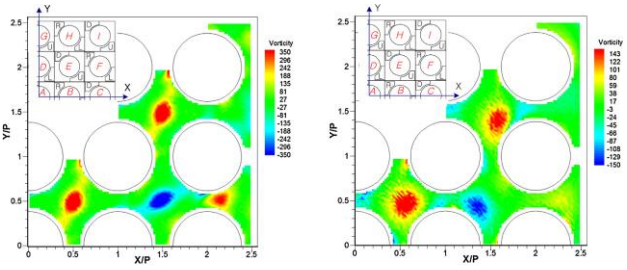

(a) Experiment [2]

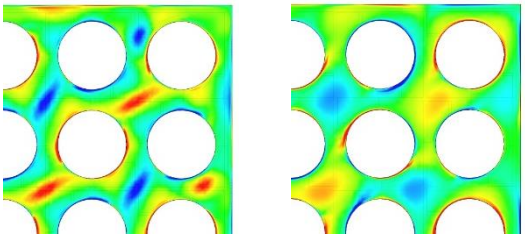

(b) Calculation (k-ε model)

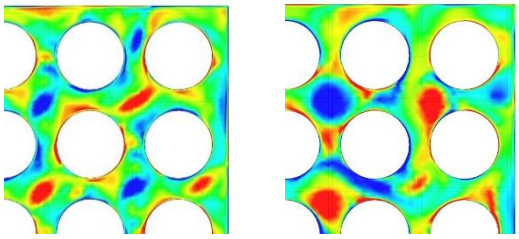

(c) Calculation (SAS-SST model)

Fig. 6. Time averaged axial vorticity contour (left : Z=1.0D_h, right : Z=10.0D_h).

3. ACOP (KAERI)

3.1 Overview of Test Facility

APR+ Core Flow & Pressure Test Facility (ACOP), installed in the KAERI, is a 1/5 scaled-down model of APR+. It consists of a reactor vessel with two coolant loops (i.e., four cold legs and two hot legs). The internal structures of the reactor model (e.g., flow skirt and

upper/lower core structures), had almost the same shapes as those in the original APR+ and satisfied geometrical similarity [5,6]. A total of 257 core simulators were installed in the reactor model. The core-inlet flow-rate distribution could be obtained by measuring the differential pressure and discharge coefficients at the venturi region of the each core simulator [5,6]. The upper head of the reactor, and some core-bypass flow-paths were neglected in the reactor model because these parts were expected to have little influence on the core-inlet flow-rate distribution [5,6]. The criteria of the allowable data scattering for each core simulator inlet flow distribution was ±1.5% [5].

3.2 Test Conditions

The test matrix consists of three flow conditions, i.e., the symmetric or asymmetric flow conditions for 4-pumps operation, and the flow condition for 3-pumps operation. In this study, CFD simulation was conducted under the symmetric flow condition for 4-pumps operation. Under this condition, the Reynolds number was about 8.6×10^5 in the downcomer.

3.3 Geometry Modeling

APR+ reactor internals are complex structures which support fuel assemblies, control rods and measuring instruments. The internal structures, especially those located in the upstream of the reactor core, may have a significant influence on the core-inlet flow-rate distribution; depending on both their shapes, and the relative distance between the internal structures and the core inlet [7]. Therefore an exact representation of these internal structures is needed for CFD simulation of the core-inlet flow-rate distribution. However, such an approach requires a great deal of computing resources to analyze the real-flow phenomena inside a reactor.

In this study, as shown in Fig. 7, among the reactor internal structures located upstream of reactor core, the real geometries of a flow skirt, lower-support-structure-bottom plate and ICI (In-Core Instrumentation) nozzle support plate, were considered because these internal structures could significantly influence the flow-rate distribution at the core inlet.

Meanwhile, to reduce total numbers of elements and thus minimize the required amount of computation, fuel assemblies and some internal structures (e.g., control-element guide tubes) were simply considered as each bulk volume (porous domain). Then, in order to reflect the velocity field and pressure drop occurring in the real-flow region; porosity and Isotropic Loss Models [4] were applied to the porous domain.

Porosity is the ratio of the volume of fluid region to total volume; including both fluid and solid regions. It has an effect on flow acceleration in the porous domain. In this study, the porosity was determined by considering the real geometry of the reactor internal structures. A momentum source was used to model the momentum loss in the porous domain; which corresponds to a pressure drop in real reactor vessel. Loss coefficients were adjusted to match the magnitude of the pressure drop found in the porous domain, with those of the measurement.

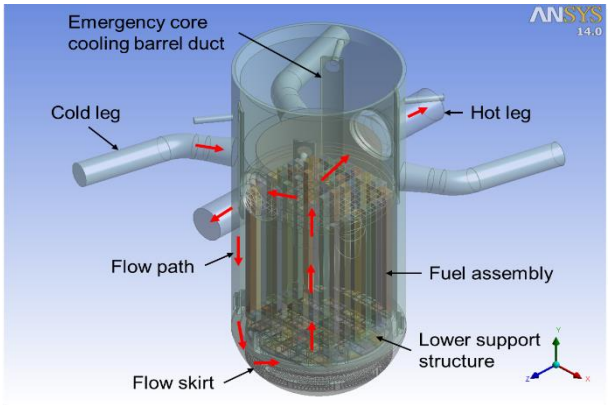

(a) Full geometry

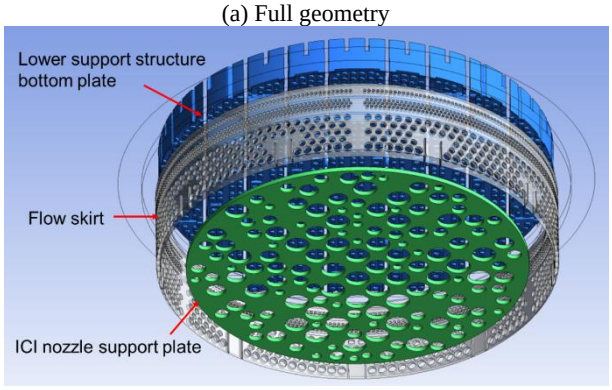

(b) Details of lower support structure

Fig. 7. The computational domain.

3.4 Numerical Modeling

3.4.1. Numerical method.

The flow inside the scaled-down APR+ model was assumed to be steady, incompressible, isothermal and turbulent. Spatial discretization errors result from both the numerical order of accuracy of the discretization scheme, and from grid spacing. In this study, a high resolution scheme was used for the convection-terms-of-momentum and -turbulence equations. The solution was considered 'converged' when the residuals of the variables were below 6×10^{-4}, and the variations of the target variables were small. Simulation was conducted with the commercial CFD software, ANSYS CFX R.14.

3.4.2. Turbulence models.

Both k-ε model and SSG (Speziale, Sarkar and Gatski) Reynolds Stress model were used to simulate the turbulent flow inside the scaled-down APR+. The SSG model is the variety of the standard Reynolds stress models based on the ε-equation available and uses a

quadratic relation for the pressure-strain correlation. More detailed descriptions of the above-mentioned turbulence models can be found in the ANSYS CFX-solver modeling guide [4].

3.4.3. Grid systems.

A hybrid mesh, made up of tetrahedrons, pyramids and prisms, was generated to prevent the oversimplification of the geometry, and to have more efficient mesh distribution. Prism layers were used to get higher resolution in the near-wall region. Total numbers of elements were 7.3×10^7. Maximum value of y+ at the downcomer was 305.

3.4.4. Boundary conditions.

By referring to the test condition [5]; an inlet flow-rate of 135 kg/s was imposed at each cold leg. Turbulence intensity at the inlet was assumed to be 5 %. Light water at 60℃ was used as the working fluid. The 'average pressure over the whole outlet' option; with a relative pressure of 0 Pa, was used at each hot leg as an outlet-boundary condition. A no-slip condition was applied at the solid wall. To model the flow in the near-wall region, scalable wall functions were applied.

3.5 Results and Discussion

Fig. 8 shows distribution of the normalized core-inlet mass-flow rate along the core centerline (A-A'). With the aid of a flow skirt, a lower-support-structure-bottom plate controls the mass-flow rate distribution at core inlet. In the experiment [5,6], a relatively high inlet-mass flow-rate was found in the core outer boundary because the size of the flow holes in the lower-support-structure-bottom plate increased in this region. The average difference between calculations with the k-ε/SSG model and measurement was 8.6%, and 11.7%, respectively. The k-ε model showed the best agreement with the measurement.

Meanwhile, the measured mass-flow rate at core-inlet plane was in the range of 86~126% of the averaged fuel assembly mass-flow rate [5]. The k-ε/SSG model predicted core-inlet mass-flow rates in the range of 79~148% and 59~145%, respectively. Although there was a little difference between measurement and prediction, the k-ε model showed the best agreement with the measurement.

4. Conclusions

In this study, to assess the applicability of k-ε model to the typical nuclear safety problems such as the complex flow phenomena inside either the fuel assembly or the reactor vessel, simulation was performed using the commercial CFD software, ANSYS CFX R.14 [1] and the predicted results with k-ε model were compared with the measured data and the computational results with more complex turbulence models. The major conclusion can be summarized as follows:

(1) Complex flow pattern inside either the fuel assembly or the reactor vessel was locally different depending on turbulence models.

(2) Prediction performance of k-ε model was at least equivalent to that of more complex turbulence models such as SSG Reynolds Stress model and SAS-SST model.

(3) Turbulence models are one of the main factors providing the uncertainties in the simulation of the typical nuclear safety problems. Therefore licensing applicants should validate the appropriate selection of the turbulence models when they use the computational result of the typical nuclear safety problems as the base data of a licensing document.

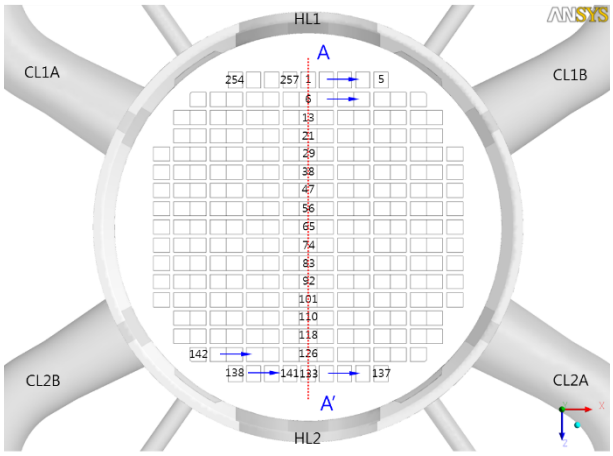

(a) Numbering of fuel assemblies

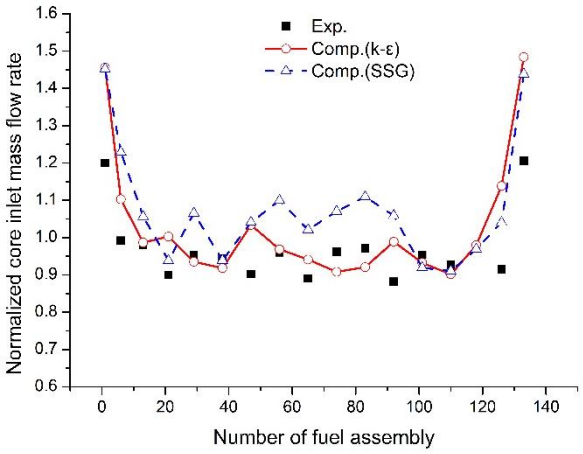

(b) Normalized core inlet mass flow rate

Fig. 8. Distribution of the normalized core inlet mass flow rate along core centerline (A-A′).

ACKNOWLEDGEMENT

This work was supported by the Nuclear Safety Research Program through the Korea Radiation Safety Foundation (KORSAFe) and the Nuclear Safety and Security Commission (NSSC), Republic of Korea (Grant No. 1305002). The authors gratefully thank Dr. Song, Dr.

Jang and Dr. Lee in the KAERI for providing the MATiS-H experimental data and giving the valuable comments.

REFERENCES

[1] ANSYS CFX, Release 14.0, ANSYS Inc.
[2] S.-K. Chang, S. Kim, C.-H. Song, Turbulent Mixing in a Rod Bundle with Vaned Spacer Grids: OECD/NEA−KAERI CFD Benchmark Exercise Test, Nuclear Engineering and Design, Vol. 279, p.19, 2014.
[3] G. H. Lee and A. J. Cheong, Effect of the Accuracy Order of the Discretization Scheme on the Prediction Performance for the Turbulent Flow Structure inside Fuel Assembly: Sensitivity Study, AJK2015-03027, Proceedings of the ASME-JSME - KSME Joint Fluids Engineering Conference 2015, July 26-31, 2015, Seoul, Korea.
[4] ANSYS CFX-Solver Modeling Guide, ANSYS Inc., 2011.
[5] D. J. Euh, K. H. Kim, J. H. Youn, J. H. Bae, I. C. Chu, J. T. Kim, H. S. Kang, H. S. Choi, S. T. Lee, T. S. Kwon, A Flow and Pressure Distribution of APR+ Reactor under the 4-Pump Running Conditions with a Balanced Flow Rate, Nuclear Engineering and Technology, Vol.44, p.735, 2012.
[6] K. H. Kim, D. J. Euh, I. C. Chu, Y. J. Youn, H. S. Choi, T. S. Kwon, Experimental Study of the APR+ Reactor Core Flow and Pressure Distributions under 4-Pump Running Conditions, Nuclear Engineering and Design, Vol.265, p.957, 2013.
[7] B. J. Lee, H. C. Jang, J. S. Cheong, S. J. Baek, Y. S. Park, A Review on the Regionalization Methodology for Core Inlet Flow Distribution Map, J. Korean Nuclear Society, Vol.33, p. 441, 2001.